Journal of Ethnopharmacology 128 (2010) 438–445

Contents lists available at ScienceDirect

Journal of Ethnopharmacology

journal homepage: www.elsevier.com/locate/jethpharm

Ophiopogonin D prevents H_2O_2-induced injury in primary human umbilical vein endothelial cells

Jinchun Qian[a,1], Fengrong Jiang[b,1], Bin Wang[a], Yang Yu[a], Xu Zhang[b], Zhimin Yin[a], Chang Liu[a,*]

[a] Jiangsu Key Laboratory for Molecular and Medical Biotechnology, College of Life Sciences, Nanjing Normal University, #1 Wenyuan Rd, Nanjing, China
[b] College of Pharmacy, Nanjing University of Traditional Chinese Medicine, Nanjing, China

ARTICLE INFO

Article history:
Received 20 August 2009
Received in revised form 8 December 2009
Accepted 11 January 2010
Available online 18 January 2010

Keywords:
Endothelial injury model
Ophiopogonin D
Oxidative stress
Inflammation
Apoptosis

ABSTRACT

Aim of the study: Vessel endothelium injury caused by reactive oxygen species (ROS) including H_2O_2 plays a critical role in the pathogenesis of cardiovascular disorders. Therefore, drug targeting ROS elimination has highly clinical values in cardiovascular therapy. The plant of *Radix Ophiopogon japonicus* is a traditional Chinese herbal medicine that has been commonly used for prevention and treatment of cardiovascular diseases for a long history. However, the effective component mediating its beneficial effects remains unknown. In the present study, we investigated the action of Ophiopogonin D (OP-D), one of the most bioactive components of *Radix Ophiopogon japonicus*, in an endothelial injury model induced by H_2O_2.
Materials and methods: Primarily cultured human umbilical vein endothelial cells (HUVECs) were pretreated with increased doses of OP-D overnight and then challenged with H_2O_2. The protective effects of OP-D against H_2O_2 were evaluated.
Results: We found that OP-D inhibited mRNA levels of antioxidant, inflammatory and apoptotic genes in a dose-dependent manner in HUVECs. H_2O_2-induced lipid peroxidation and protein carbonylation were reduced by OP-D pretreatment. Mitochondrial ROS generation and cell apoptosis were also attenuated in OP-D pretreated cells. In addition, OP-D restored cellular total antioxidative capacity and inhibited the release of inflammatory cytokines. Furthermore, OP-D suppressed the enzymatic activity of catalase, HO-1, and caspases. Finally, OP-D blocked activation of NF-κB and ERK signaling cascades.
Conclusion: Our findings provide the first evidence that OP-D plays a protective role as an effective antioxidant in H_2O_2-induced endothelial injury. Ophiopogonin D can be therefore developed as a novel drug for the therapy of cardiovascular disorders.

1. Introduction

Chronic increased oxidative stress is a pathogenic feature of cardiovascular diseases such as atherosclerosis, restenosis, hypertension, diabetic vascular complications and heart failure (Cai and Harrison, 2000). Oxidative stress is mainly caused by the excessive accumulation of reactive oxygen species (ROS), which include H_2O_2, superoxide anions, and hydroxyl radicals. Among them, H_2O_2, the major source of endogenous ROS (Nohl et al., 2003), is generated during hypoxia and ischemia-reperfusion injury (Hashimoto et al., 1994), and has been extensively used to induce oxidative stress in *in vitro* models (Yang et al., 2006).

Under pathological conditions, vascular NAD(P)H oxidases are activated by agonists and subsequently activate xanthine oxidase or uncouple eNOS, which in turn produce H_2O_2 in large quantities (McNally et al., 2003). In contrast to stimulating endothelial cell growth and proliferation at ambient levels, large amount of H_2O_2 leads to detrimental consequences including cell apoptosis and inflammation by modulating a series of intracellular signaling pathways (Zafari et al., 1998). Among these pathways, the activation of mitogen-activated protein kinase (MAPK) cascade is known to play major roles in cell growth, survival, differentiation, and apoptosis responses (Yang et al., 2004). Therefore, high levels of H_2O_2 contribute importantly to endothelial dysfunction and the development of vascular diseases.

The plant of *Radix Ophiopogon japonicus* is a traditional Chinese herbal medicine that has been commonly used to treat inflammatory and cardiovascular diseases for thousands of years (Kou et al., 2006). Extensive studies revealed that *Ophiopogon japonicus* has remarkable anti-inflammatory property and beneficial cardiovascular effects, such as anti-ischemia, anti-arrhythmic, inhibiting platelet aggregation, protecting endothelium from apoptosis, improving microcirculation, and so on (Kou et al., 2005). However, the effective component mediating its beneficial effects

* Corresponding author. Tel.: +86 25 85891870; fax: +86 25 85891870.
E-mail addresses: changliu@njnu.edu.cn, liuchang770202@yahoo.com.cn (C. Liu).
[1] These authors contributed equally to this work.

0378-8741/$ – see front matter © 2010 Elsevier Ireland Ltd. All rights reserved.
doi:10.1016/j.jep.2010.01.031

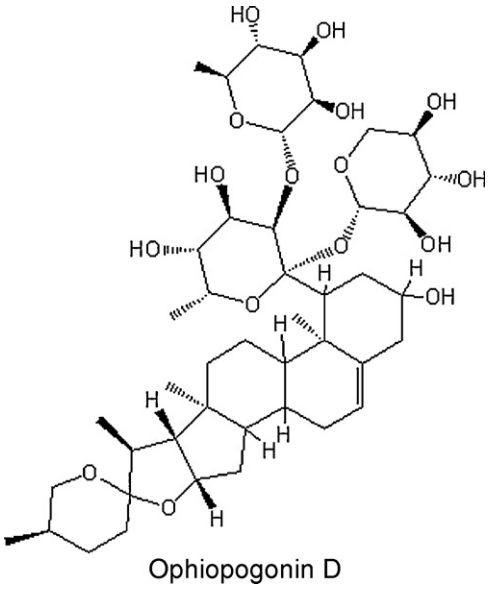

Fig. 1. Chemical structure of Ophiopogonin D (OP-D).

remains unidentified. Ophiopogonin D (OP-D) (Fig. 1) is a steroidal glycoside recently isolated from *Ophiopogon japonicus*. Previous studies demonstrated that OP-D has various biological properties, including inhibition of venous thrombosis (Kou et al., 2006), anti-inflammation (Kou et al., 2005), and antitussive activity (Takahama and Miyata, 1995). The aim of study was to investigate the effects of OP-D on H_2O_2-induced endothelial cell injury to further extend our understanding of the pharmaceutical functions of OP-D and to provide experimental evidence for its potential clinical use in the treatment of cardiovascular diseases.

2. Materials and methods

2.1. Reagents and antibodies

OP-D was purchased from Tsumura (Tokyo, Japan) and was first dissolved in DMSO at a concentration of 5 mM. This master solution was further diluted to the final concentration in the culture medium. Trizol reagent was obtained from Invitrogen (Carlsbad, USA). Endothelial cell growth supplement (ECGS) was from Becton–Dickinson (Bedford, USA). Collagenase type IV was from Pharmacia (Uppsala, Sweden). OxiSelect protein carbonyl immunoblot kit was from Cell Biolabs (San Diego, USA). SYBR-Green Master Mix was from Applied Biosystems (Foster City, USA). Reduced MitoTracker Red probe (CM-H2XRos) was from Molecular Probes (Eugene, USA). Hoechest 33258 staining solution, lipid peroxidation MDA assay kit, enzymatic activity assay kits for catalase, caspase-3, and caspase-9 were from Beyotime Biotechnology (Nantong, China). Kit for total antioxidative capacity (T-AOC) analysis was from Jiancheng Bioengineering Institute (Nanjing, China). Kits for TNF-α and IL-6 measurement were from Sino-UK Institute of Biological Technology (Beijing, China). Nuclear and cytoplasmic extraction kit was from BestBio (Shanghai, China). Monoclonal antibody against Factor VIII was from Sigma (St. Louis, USA). Antibodies against NF-κB p65 subunit, Histone H1 and GAPDH were from Santa Cruz (Santa Cruz, USA). Phospho-specific anti-ERK1/2 and anti-total ERK1/2 antibodies were from Cell Signaling (Danvers, USA). CellTiter-Glo luminescent cell viability assay kit was from Promega (Madison, USA). All other reagents were of analytical grade.

2.2. HUVECs culture

Human umbilical vein endothelial cells (HUVECs) were isolated from umbilical vein cords of normal pregnancies as described previously (Muñoz et al., 1996). These cells were cultured on flasks coated with 0.2% gelatin in M199 medium supplemented with 10% FBS, 50 mg/L ECGS, 25 mM HEPES (pH 7.4), 100 U/mL penicillin, 100 mg/mL streptomycin, 50 μg/mL heparin, and 2 mM glutamine in an atmosphere of 5% CO_2 at 37 °C. The medium was changed every 3 days until the cells reached confluence. HUVECs were identified by the characteristic "cobble stone" growth pattern and positive immunocytochemical staining with a monoclonal antibody against Factor VIII. To maintain uniform condition, all experiments were carried out between cell passages 2 and 3. To assess the effect of OP-D on cellular oxidative stress, we pretreated cells with increased concentrations of OP-D (0.6, 6.0, and 60.0 μM) overnight in serum-free medium. The cells were washed twice and then challenged with 300 μM H_2O_2 for 2 h unless indicated otherwise. The purpose of washing was to eliminate any possible interaction of OP-D and H_2O_2.

2.3. Lipid peroxidation and protein carbonylation assay

For lipid peroxidation assay, we used a commercial kit to quantify the generation of malondialdehyde (MDA) according to the manufacturer's protocol. In brief, cells were harvested by trypsinization and cellular extracts were prepared by sonication in ice-cold buffer (50 mM Tris–HCl, pH 7.5, 5 mM EDTA, and 1 mM DTT). After sonication, lysed cells were centrifuged at 10,000 × *g* for 20 min to remove debris. The supernatant was subjected to the measurement of MDA levels and the protein contents. We used a protein assay kit (Bio-Rad Laboratories, Hercules, USA) to quantify protein concentration. MDA levels were then normalized to milligram protein. We used the same procedure to lyse the cells and determine the protein contents in the following assays unless otherwise indicated.

Carbonylated proteins were detected using the OxiSelect kit. Briefly, cells were lysed and 20 μg of proteins were reacted with 2,4-dinitrophenylhydrazine (DNPH) for 5 min at 25 °C. Samples were resolved on 12% denaturing polyacrylamide gels, and DNP-derivatized proteins were identified by immunoblot using an anti-DNP antibody.

2.4. Real-time RT-PCR

Total RNA from HUVECs was extracted by using Trizol reagent according to the manufacturer's protocol. Two micrograms of total RNA was reverse-transcribed into complementary DNA and β-actin served as an internal control for total complementary DNA content. mRNA levels of interested genes were quantified by real-time RT-PCR using SYBRGreen Master Mix. Specific primers were used for pgc-1α (sense: 5′-TCAGTCCTCACTGGTGGACA-3′, antisense: 5′-TGCTTCGTCGTCAAAAACAG-3′); catalase (sense: 5′-CGCAGAAAGCTGATGTCC TGA, antisense: 5′-TCATGTGTGACCTCAAAGTAGC-3′); HO-1 (sense: 5′-GTCTTCGCCCCTGTC TACTTC-3′, antisense: 5′-CTGGGCAATCTTTTTGAGCAC-3′); TNF-α (sense: 5′-ATGAGCACTGAA AGCATGATCC-3′, antisense: 5′-GAGGGCTGATTAGAGAGAGGTC-3′); IL-6 (sense: 5′-AAATTC TACATCCTCGACGG-3′, antisense: 5′-GGAAGGTTCAGGTTGTTTTCTGC-3′); NF-κB p65 subunit (sense: 5′-GGGGACTACGACCTGAATG-3′, antisense: 5′-GGGCACGATTGTCAAAGAT-3′); caspase-3 (sense: 5′-ATGGAAGCGAATCAATGGACTC-3′, antisense: 5′-CTGTACCAGACCGAG ATGTCA-3′); caspase-9 (sense: 5′-GGCTGTCTACGGCACAGATGGA-3′, antisense: 5′-CTGGCT CGGGGTTACTGCCAG-3′); β-actin (sense: 5′-CACCCACACTGTGCCCATCTACGA-3′, antisense: 5′-CAGCGGAACCGCTCATTGCCAATGG-3′).

2.5. Enzymatic activity analysis

We quantified enzymatic activity of catalase, caspase-3, and caspase-9 using commercial assay kits according to the manufacturer's protocols. The rate of change in absorbance was converted to units of enzyme activity, determined from a standard curve. Enzyme activity was then standardized to milligram protein. HO-1 activity was evaluated by assaying bilirubin production. In brief, cells were lysed and 40 μL of protein lysates were incubated with freshly prepared 2 mM hemin and 4.5 mM NADPH (final reactant concentrations 41.67 μM hemin, 93.75 μM NADPH, total volume 1920 μL); control samples lacked NADPH. Reactions were then run for 10 min at 37 °C in a dark place, and were terminated by quick-freezing vials on dry ice. The samples were scanned with a spectrophotometer (BioTek Synergy 2, Vermont, USA) at absorbance from 464 to 530 nm. Bilirubin concentration was calculated based on the change of optical density from 530 to 464 nm, with an extinction coefficiency of 40 $mmol^{-1}$ cm^{-1}. HO-1 activity was expressed as micromole of bilirubin per milligram of protein per hour (μmol bilirubin/(mg protein/h)).

2.6. Western blotting analysis

HUVECs were lysed in RIPA's buffer containing 50 mM Tris/HCl (pH 8.0), 150 mM NaCl, 1% Nonidet-P40, 1% sodium deoxycholate, 0.1% SDS, 0.1 mM DTT, 0.05 mM PMSF, 0.002 mg/mL aprotinin, 0.002 mg/mL leupeptin, and 1 mM $NaVO_3$. Equal amounts of protein were loaded and separated by 10% SDS-PAGE and then transferred onto polyvinylidene difluoride membrane. The membranes were incubated overnight with appropriate primary antibodies. Bound antibodies were then visualized using alkaline phosphatase-conjugated secondary antibodies. Quantitative analysis was performed by NIH Image J 1.32j software. For the detection of translocation of NF-κB p65 protein to the nucleus, we firstly prepared nuclear and cytoplasmic protein using a commercial extraction kit and then performed Western blotting analysis as mentioned above. We used GAPDH and Histone H1 as the loading control for the cytoplasmic and nuclear protein, respectively.

2.7. Measurement of mitochondrial ROS

To evaluate the direct production of mitochondrial ROS in HUVECs, specific staining with the reduced MitoTracker Red probe (CM-H2XRos) was performed. In brief, cells were grown on gelatin-coated cover slides and loaded with 20 μM CM-H2XRos at 37 °C for 15 min. A fluorescence microscope (AxioCam MRc5, Carl Zeiss) equipped for equifluorescent illumination was used.

2.8. Hoechest 33258 staining

HUVECs were collected, washed with PBS buffer and fixed with 10% formaldehyde at room temperature for 10 min. Following centrifugation, the samples were washed with PBS three times, stained with Hoechest 33258 staining solution in the dark for 5 min and then seeded separately onto cover slides. Once the treated samples had been dried in the dark, stained nuclei were observed under a fluorescence microscope.

2.9. Fluorescence-activated cell sorting (FACS) analysis

HUVECs were subjected to single parameter analysis for apoptosis and DNA fragmentation. In brief, cells were washed with PBS and suspended in 100% ethanol at 4 °C overnight. Fixed cells were then collected and the nuclei were stained for 30 min at 4 °C with hypotonic fluorochrome solution, containing 0.1% sodium citrate, 0.1% Triton-X-100 and 50 mg/mL propidium iodide (PI). After extensively washing, the PI fluorescence of individual nuclei was measured by a FACSort flow cytometer (Becton–Dickinson, San Jose, USA). DNA content was analyzed and sub-G1 population was obtained as an indicator of apoptosis.

2.10. Detection of T-AOC and cytokine release

The T-AOC values of the cells were measured with an analysis kit. This kit utilized antioxidants in the samples to reduce Fe^{3+}–Fe^{2+}, which was then chelated with porphyrin to produce a purple complex; this was quantified by measuring the absorbance at 550 nm. The relative T-AOC values of the samples were normalized to protein concentration. For the measurement of inflammatory cytokine release, culture medium was collected and briefly centrifuged. The levels of TNF-α and IL-6 in the supernatant were determined using radioimmunoassay (RIA) and the corresponding commercial kits.

2.11. Cell viability assay

Cell viability was determined by the quantitation of the ATP present, which signals the presence of metabolically active cells, by using CellTiter-Glo luminescent cell viability assay kit.

2.12. Data analysis

All data are presented as mean ± SEM. Data were analyzed using a one-way ANOVA followed by Fisher's LSD post hoc test. Calculations were performed using SPSS/Windows version 12.5S statistical package (SPSS, Chicago, USA). In all cases $P < 0.05$ was taken as statistically significant.

3. Results

3.1. OP-D prevents H_2O_2-induced oxidative stress in HUVECs

We first determined the effects of OP-D on mitochondrial ROS production in HUVECs. As shown in Fig. 2A, MitoTracker Red fluorescence in HUVECs significantly increased with 300 μM H_2O_2, compared with the control. H_2O_2-induced fluorescence was dose-dependently suppressed by pretreatment with OP-D, indicating the abolishment of mitochondrial ROS production.

Cellular T-AOC is regulated by external stimuli and reflects the antioxidant ability of the drug. In H_2O_2-stimulated HUVECs, T-AOC was suppressed to 42.1% compared with the control (Fig. 2B). However, preincubation of cells with OP-D restored T-AOC in a dose-dependent manner. Overnight treatment with 60.0 μM OP-D almost completely recovered cellular T-AOC.

Intracellular antioxidant defense consists of several key enzymes (e.g. catalase and heme oxygenase-1 (HO-1)) and is controlled by the master regulator of pgc-1α. We found H_2O_2 upregulated mRNA levels of pgc-1α, catalase, and HO-1 to 6.35-, 1.95-, and 3.53-fold, respectively (Fig. 2C). However, such inductions were suppressed by pretreatment of OP-D in a dose-dependent manner. We noticed that the effect of OP-D on the suppression of relative mRNA levels of catalase and HO-1 was not very significant, so we further explored the regulation of their enzymatic activity by OP-D. As shown in Fig. 2D, H_2O_2 increased catalase and HO-1 activity to 2.03- and 5.5-fold, respectively. In contrast, OP-D pretreatment almost completely reduced their activity to the basal levels.

One of the important aspects of damage caused by ROS, especially by H_2O_2, is the oxidation of proteins and lipids. To determine if OP-D treatment can protect the cells from these damages, we measured lipid peroxidation and protein carbonylation in HUVECs. We found that MDA generation was increased to 1.8-fold by H_2O_2

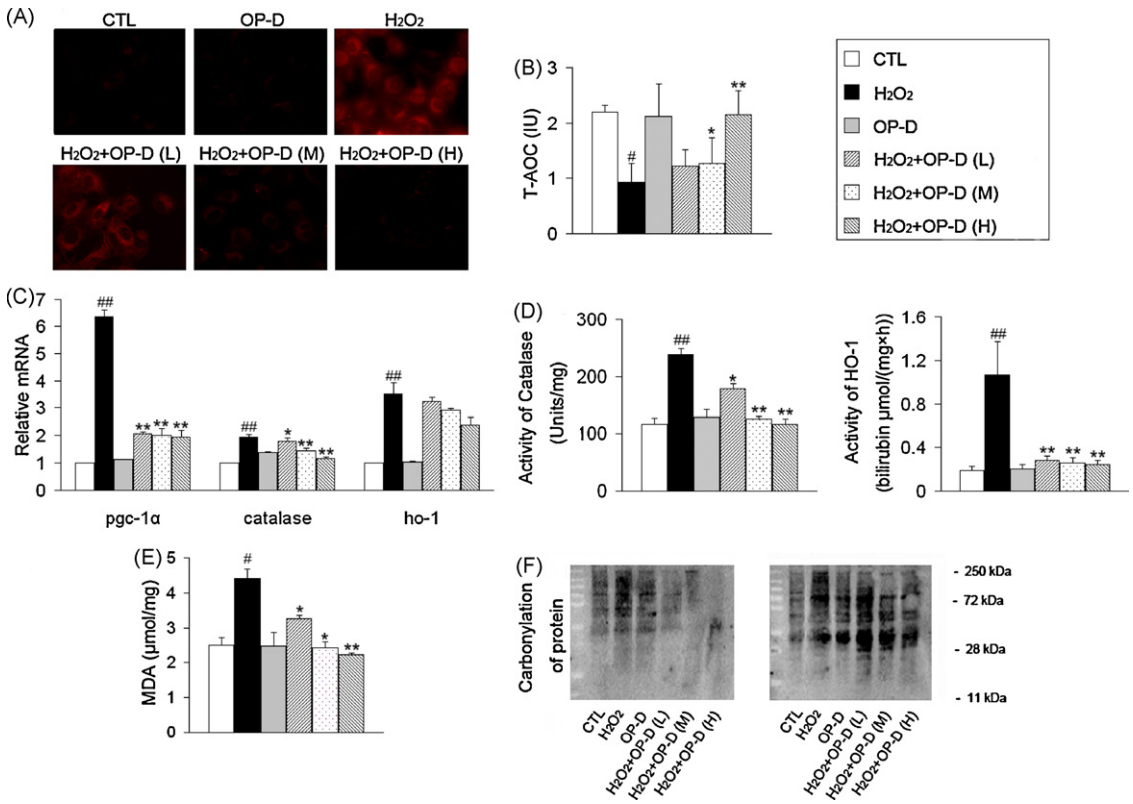

Fig. 2. Attenuation of H_2O_2-induced oxidative stress in HUVECs by OP-D. HUVECs pretreated with or without OP-D (0.60 μM (L), 6.0 μM (M), and 60.0 μM (H), the same below) overnight were stimulated with H_2O_2 (300 μM) for 2 h. (A) Mitochondrial ROS generation was detected by MitoTracker Red staining using microflurometry (fluorescence microscope, 400×). (B) Cellular T-AOC quantification. (C) mRNA quantification for pgc-1α, catalase, and HO-1 by real-time RT-PCR. (D) Enzymatic activity of catalase and HO-1. (E) Analysis of MDA generation and lipid peroxidation. (F) Analysis of protein carbonylation. For panels B to E, the data were shown as fold increase compared with control (CTL) from the mean values from five independent experiments. For panel F, representative blots from two independent experiments were shown. $^{\#\#}P < 0.01$ and $^{\#}P < 0.05$ *vs.* control (CTL); $^{**}P < 0.01$ and $^{*}P < 0.05$ *vs.* H_2O_2.

challenge, and OP-D (from 0.6 to 60 μM) inhibited MDA levels by 26.3%, 44.8%, and 50.2%, respectively (Fig. 2E). Protein carbonylation showed the similar trend. In Fig. 2F, cells were lysed and protein carbonyls were then derivatized to DNPH and detected by immunoblotting with an anti-DNP antibody. We found that H_2O_2 clearly promoted the protein carbonyl contents, which was dose-dependently attenuated by OP-D pretreatment.

3.2. OP-D inhibits H_2O_2-induced inflammation in HUVECs

Inflammation is one of the accompanied consequences caused by oxidative stress. To investigate whether OP-D can protect cells from inflammation, we performed RIA analysis to quantify inflammatory cytokines released to culture medium. As shown in Fig. 3A, 2 h incubation with H_2O_2 increased the release of TNF-α and IL-6 to 2.67- and 1.67-fold, respectively. OP-D pretreatment suppressed the cytokine release, although the extent was not significant.

Similar trends were observed in mRNA expression levels. Real-time RT-PCR analysis indicated that H_2O_2-induced mRNA levels of TNF-α, IL-6, and NF-κB p65 subunit to 8.14-, 4.77-, and 1.53-fold, respectively (Fig. 3B), while OP-D reduced the expression of such genes. Note that the mRNA levels of these genes declined to the basal level with the preincubation of 60.0 μM OP-D.

It is known that NF-κB plays a key role in the transcriptional regulation of many proteins involved in inflammatory responses. The activation of NF-κB signaling pathway includes the translocation of NF-κB from cytoplasm to the nucleus and the phosphorylation of its subunits. To further determine if OP-D can block the activation of NF-κB induced by H_2O_2, we examined the cellular localization of the p65 subunit. As is usually observed in unstimulated cells, NF-κB is localized mainly in the cytoplasm with only minor nuclear staining detected. Stimulation of cells by H_2O_2-induced p65 translocation from the cytoplasm into the nucleus, indicative of the NF-κB activation. In contrast, pretreatment of cells with OP-D nearly completely blocked the nuclear translocation of p65 (Fig. 3C).

3.3. OP-D attenuates H_2O_2-induced apoptosis in HUVECs

Hoechest 33258 staining assay showed that apoptotic bodies containing nuclear fragments were significantly generated in H_2O_2-treated cells (Fig. 4A). However, pretreatment of OP-D reduced cell apoptosis and 60 μM of OP-D almost completely abolished the pro-apoptotic action of H_2O_2 (Fig. 4A). Fluorescence results were confirmed by using FACS analysis. As shown in Fig. 4B, a sub-G1 population (62.2%) associated with apoptotic cells appeared in H_2O_2-treated cells. By contrast, increased doses of OP-D (from 0.6 to 60.0 μM) reduced the percentage of apoptotic cells to 44.0%, 36.1%, and 28.2%, respectively.

The protective effect of OP-D on apoptosis prompted us to investigate whether OP-D reduces the activation of the classic mitochondrial apoptosis cascade, which involves the sequential mRNA induction/activation of caspase-3 and caspase-9. As shown in Fig. 4C, mRNA levels of caspase-3 and caspase-9 were increased to 2.41- and 1.92-fold by H_2O_2 challenge. However, OP-D downregulated their mRNA levels by 20.8%, 31.7%, and 38.5% for caspase-3 and 30.9%, 31.6%, and 43.2% for caspase-9. These findings suggest that OP-D blocks activation of the mitochondrial apoptosis cascade at least partially through transcriptional regulation.

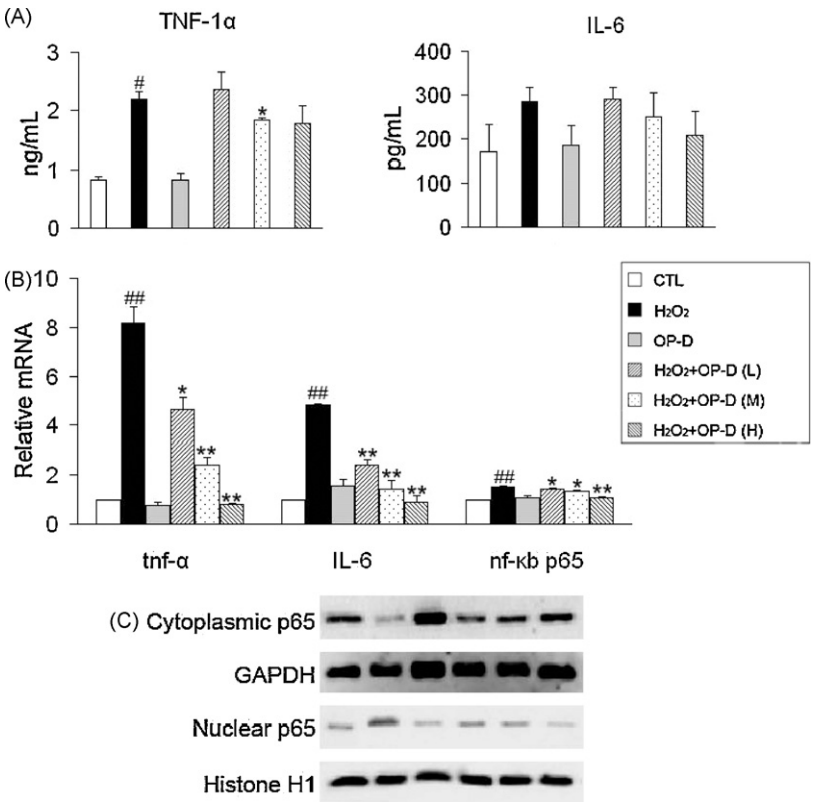

Fig. 3. Inhibition of H_2O_2-induced inflammation in HUVECs by OP-D. HUVECs were treated under the same experimental conditions described as in Fig. 2. (A) Culture medium was collected and the levels of TNF-α and IL-6 were determined using RIA. (B) mRNA quantification for TNF-α, IL-6, and NF-κB by real-time RT-PCR. (C) Cellular localization of NF-κB p65 subunit. The data from five different experiments were calculated and plotted the same as in Fig. 2. $^{\#}P < 0.05$ *vs.* control (CTL); $^{*}P < 0.05$ *vs.* H_2O_2.

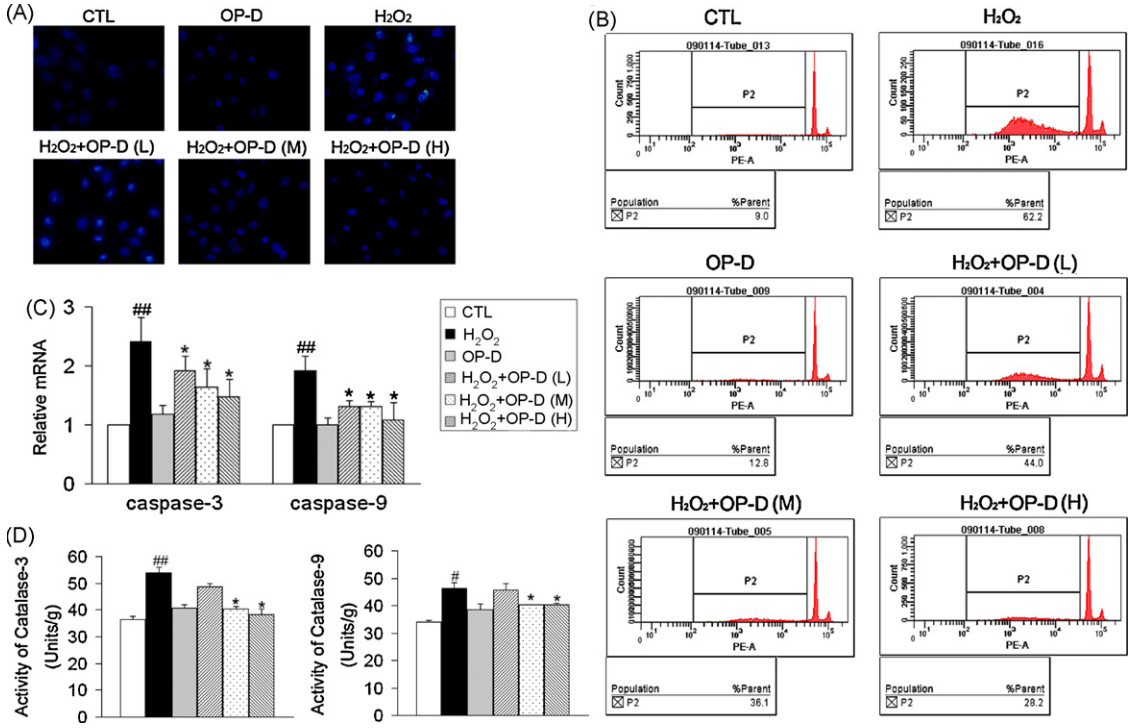

Fig. 4. Inhibition of H_2O_2-induced apoptosis in HUVECs by OP-D. HUVECs were treated under the same experimental conditions described as in Fig. 2. (A) Hoechest 33258 staining of the cells (fluorescence microscope, 400×). (B) Representative FACS profiles. "P2" indicated the area of sub-G1 population. (C) mRNA quantification for caspase-3 and caspase-9 by real-time RT-PCR. (D) Enzymatic activity of caspase-3 and caspase-9. The data were calculated and plotted the same as in Fig. 2. $^{\#\#}P < 0.01$ and $^{\#}P < 0.05$ *vs.* control (CTL); $^{*}P < 0.05$ *vs.* H_2O_2.

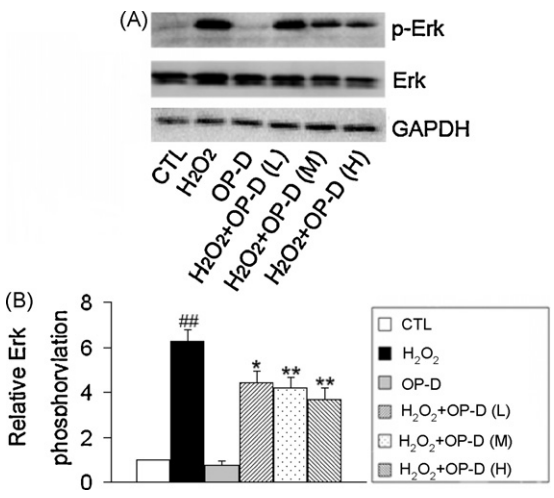

Fig. 5. Inhibition of H_2O_2-induced ERK1/2 activation in HUVECs by OP-D. HUVECs pretreated with or without OP-D overnight were stimulated with H_2O_2 (30 μM) for 15 min. Then cells were harvested and lysed, and the ERK1/2 activation was measured by immunoblot using phospho-specific anti-ERK1/2 antibodies. (A) Representative blots with phospho-specific anti-ERK1/2 (up panel) and total anti-ERK1/2 (bottom panel) antibodies. (B) The signal ratio of phospho ERK1/2 to total ERK1/2 was quantified by densitometric scanning. The data from three different experiments were calculated and plotted the same as in Fig. 2. $^{\#}P < 0.05$ *vs.* control; $^{*}P < 0.05$ *vs.* H_2O_2.

We next measured the enzymatic activity of these caspases. There was a 149%/136% elevation of caspase-3/-9 activity following 2 h treatment with 300 μM of H_2O_2. Such activity induction was slightly but still significantly reduced by OP-D (Fig. 4D).

3.4. OP-D inhibits ERK1/2 activation stimulated by H_2O_2

It has been well recognized that ROS generation is linked to the activation of ERK/MAPK signaling cascade. Therefore, we reasoned that the antioxidant effect of OP-D might modulate redox-sensitive ERK1/2 in HUVECs. Because ERK1/2 activation by H_2O_2 (30 μM), as measured by immunoblotting, was detectable as early as 5 min and peaked at 15 min (data not shown), we examined the effect of OP-D on ERK1/2 activation at 15 min after H_2O_2 (30 μM) stimulation using phospho-specific anti-ERK1/2 antibodies. As shown in Fig. 5, OP-D inhibited H_2O_2-induced ERK1/2 activation in a dose-dependent manner, suggesting that the action of OP-D is via a redox-sensitive pathway.

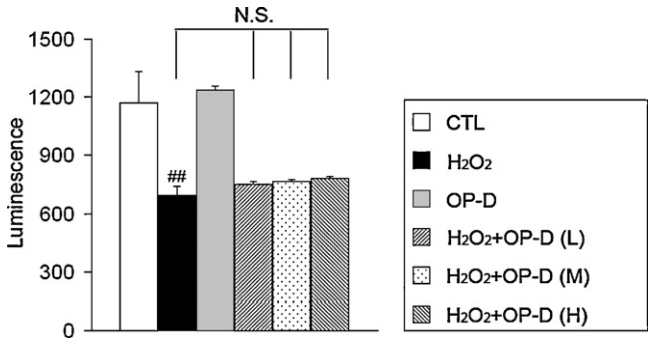

Fig. 6. OP-D moderately increases the cell viability. HUVECs were treated under the same experimental conditions described as in Fig. 2 and the viable cells were determined using CellTiter-Glo luminescent cell viability assay kit. The data from three different experiments were calculated and plotted the same as in Fig. 2. $^{\#\#}P < 0.01$ *vs.* control (CTL); N.S., no significant difference.

3.5. OP-D moderately increases the cell viability

To rule out the possibility that the suppressive effect of OP-D on pro-inflammatory cytokines release is due to the suppression of cell growth, we evaluated the influence of OP-D to the growth of HUVECs. As shown in Fig. 6, H_2O_2 caused the cell death and the number of the viable cells in H_2O_2-treated group was only 59% compared with the control. And OP-D moderately increased cell viability, although the extent did not reach to the significant difference.

4. Discussion

It has been well established that the elevated release of ROS from vessel tissue under pathological conditions is a fundamental mechanism leading to the endothelial injury (such as inflammation and apoptosis). Protection of endothelial cells from ROS-induced injury may therefore provide beneficial therapeutical intervention to successfully combat cardiovascular diseases. In the present study, we demonstrated for the first time that OP-D was capable of protecting HUVECs from oxidative stress and the accompanied inflammatory responses and apoptosis caused by H_2O_2. Its effects are possibly achieved via ERK pathway. These findings suggest that OP-D may have therapeutical use in the prevention of cardiovascular diseases.

Under normal conditions, significant amounts of ROS including H_2O_2 are produced in the course of oxygen metabolism. ROS-induced oxidative stress activates endogenous antioxidant defense in which transcriptional coactivator PGC-1α plays a dominant role (St-Pierre et al., 2006). Here, we found mRNA levels of PGC-1α, catalase and HO-1 were elevated by H_2O_2. Catalase is a ferri- or manganese-containing antioxidant enzyme and functions in the detoxification of H_2O_2 (Matés and Sánchez-Jiménez, 1999). And HO-1 is the rate-limiting enzyme involved in the conversion of heme into biliverdin (antioxidant), carbon monoxide (vasodilatory, anti-inflammatory, anti-mitogenic, and anti-apoptotic) and free iron (Ryter et al., 2006). The observation of the elevation of antioxidant genes is coincided with previous reports (Varani et al., 1992; Han et al., 2009) and suggests that compensatory induction of antioxidant defense is initiated to antagonize the heavier oxidative burden. We also found that OP-D pretreatment both decreased mitochondrial ROS generation and suppressed mRNA levels/activity of antioxidant enzymes. More importantly, OP-D reduced protein and lipid damages caused by ROS. All these observations indicate that the endogenous oxidative stress was ameliorated by OP-D. Further study is required to elucidate other pathways mediating in the inhibition of ROS generation by OP-D, such as inhibition of NADPH oxidase activity and/or activation of the ROS scavenging system. It should be noted here that OP-D did not significantly recover H_2O_2-induced the loss of cell viability in our study. We still do not know if higher concentration and/or longer incubation time of OP-D will give stronger protection.

Endothelial inflammatory responses are the major detrimental consequences of H_2O_2-induced oxidative stress. Several inflammatory cytokines are induced by H_2O_2 in endothelial cells (Cai, 2005). H_2O_2 was also shown to increase TNF-α mRNA expression in HUVECs (Valen et al., 1999), which was confirmed by our study (Fig. 3B). Therefore, H_2O_2 is a powerful pro-inflammatory factor acting in endothelial cells. In the present study, we found H_2O_2-induced inflammatory gene expression was dose-dependently suppressed by OP-D. Indeed, the anti-inflammatory property of OP-D has been revealed in the previous report, which showed that OP-D reduced phorbol-12-myristate-13-acetate (PMA)-induced adhesion of HL-60 cells to ECV304 cells (Kou et al., 2005). More

importantly, NF-κB is a critical signaling molecule in responses produced by a variety of stimuli that include growth factors, lymphokines, UV irradiation, pharmacological agents, and oxidant stress. Therefore, a potential mechanism whereby OP-D could modulate inflammatory responses to H_2O_2 is by blocking activation of the transcription factor NF-κB. In its inactive form, NF-κB is sequestered in the cytoplasm, bound by members of the I-κB family of inhibitor proteins. Phosphorylation of I-κB by an I-κB kinase complex exposes nuclear localization signals on the NF-κB subunits and induces translocation of the molecule to the nucleus. In the nucleus, NF-κB binds with consensus sequences of various genes, activating their transcription (Basak and Hoffmann, 2008). Our observations that OP-D attenuated H_2O_2-induced nuclear translocation of NF-κB suggest a likely mechanism of the anti-inflammatory effects of OP-D. To our knowledge, this is the first study to report that OP-D inhibits NF-κB activation. The molecular mechanisms leading to inhibition of NF-κB activation by OP-D remain to be determined. Finally, we noticed that although OP-D significantly retarded H_2O_2-induced mRNA expression of TNF-α and IL-6, the release of these two pro-inflammatory cytokines was only moderately inhibited by OP-D. These observations implicate that the inhibitory effects of OP-D on TNF-α and IL-6 are largely limited at the transcriptional level, rather than at the translational level and in the posttranslational secretion process.

In addition to inflammation, it is also well known that H_2O_2 induces apoptosis in HUVECs (Lin et al., 2004). Indeed, our results showed that the apoptotic cells were increased and the mRNA levels/enzymatic activity of caspases-3 and -9 were upregulated by H_2O_2 treatment. Caspases, a family of specific cysteine proteases, are critical mediators of apoptosis. Among them, caspase-3 is a primary executioner of apoptosis induced by a variety of stimuli including H_2O_2 (Boatright and Salvesen, 2003). And caspase-9 is a major activator in mitochondrial mediated apoptotic pathway responsible for caspase-3 activation (Kuida, 2000). In our study, OP-D attenuated H_2O_2-induced mRNA expression/activity of caspases-3 and -9. This reduction could be due to the consequence of antioxidation or the direct regulation of apoptotic process by OP-D. It is noted that the protective function of OP-D in apoptosis is not very powerful based on the evidence from the fluorescence data and also the inhibition of mRNA expression/activity of caspase-3/-9 is not very high after OP-D treatment. These observations suggest that OP-D mainly acts as an antioxidant drug with mild anti-apoptotic property.

Intracellular ROS has been shown to function as a second messenger to activate a set of MAPK family members, such as ERK1/2 (Watanabe et al., 2006), JNK (Lin et al., 2004), and p38 MAPK (Usatyuk et al., 2003). In the present study, the redox-sensitive ERK activation by H_2O_2 was inhibited by OP-D (Fig. 5), suggesting that the antioxidant action of OP-D is partly responsible for blockade of redox-sensitive signal transduction pathway. In addition, ERK plays an active role in apoptosis although the existing evidence regarding whether ERK is a pro-survival or a pro-apoptosis signal mediator is conflicting (Fischer et al., 2005; Yang et al., 2006; Wang et al., 2006; Liu et al., 2007). Taken together, ERK pathway may be a target of OP-D and contributes to the prevention of H_2O_2-induced cell apoptosis.

In conclusion, the present study revealed for the first time the antioxidant effects of OP-D in HUVECs. OP-D directly inhibits mitochondrial ROS generation stimulated by H_2O_2 and also inhibits H_2O_2-induced inflammatory responses and redox-sensitive signal transduction (ERK). These data strongly support to the contention that OP-D plays a protective role in H_2O_2-induced endothelial injury as a potent antioxidant. OP-D may have highly clinical values in the therapy of cardiovascular disorders.

Acknowledgements

This work was supported by grants from Chinese National Science Foundation (30870928), the Natural Science Foundation of the Jiangsu Higher Education Institutions of China (09KJA180003). Nanjing Normal University Outstanding Talents Program (2008104XGQ0065), Opening Project of Jiangsu Key Laboratory for Molecular and Medical Biotechnology (MMB09KF05), and Mega-projects of Science Research for the 11th Five-year Plan of China (2009ZX09302).

References

Basak, S., Hoffmann, A., 2008. Crosstalk via the NF-κB signaling system. Cytokine Growth Factor Reviews 19, 187–197.
Boatright, K.M., Salvesen, G.S., 2003. Mechanisms of caspase activation. Current Opinion Cell Biology 15, 725–731.
Cai, H., 2005. Hydrogen peroxide regulation of endothelial function: origins, mechanisms, and consequences. Cardiovascular Research 68, 26–36.
Cai, H., Harrison, D.G., 2000. Endothelial dysfunction in cardiovascular diseases: the role of oxidant stress. Circulation Research 87, 840–844.
Fischer, S., Wiesnet, M., Renz, D., Schaper, W., 2005. H_2O_2 induces paracellular permeability of porcine brain-derived microvascular endothelial cells by activation of the p44/42 MAP kinase pathway. European Journal of Cell Biology 84, 687–697.
Han, Z., Varadharaj, S., Giedt, R.J., Zweier, J.L., Szeto, H.H., Alevriadou, B.R., 2009. Mitochondria-derived reactive oxygen species mediate heme oxygenase-1 expression in sheared endothelial cells. The Journal of Pharmacology and Experimental Therapeutics 329, 94–101.
Hashimoto, Y., Itoh, K., Nishida, K., Okano, T., Miyazawa, Y., Okinaga, K., 1994. Rapid superoxide production by endothelial cells and their injury upon reperfusion. The Journal of Surgical Research 57, 693–697.
Kou, J., Sun, Y., Lin, Y., Cheng, Z., Zheng, W., Yu, B., Xu, Q., 2005. Anti-inflammatory activities of aqueous extract from radix ophiopogon japonicus and its two constituents. Biological & Pharmaceutical Bulletin 28, 1234–1238.
Kou, J., Tian, Y., Tang, Y., Yan, J., Yu, B., 2006. Antithrombotic activities of aqueous extract from radix ophiopogon japonicus and Its Two Constituents. Biological & Pharmaceutical Bulletin 29, 1267–1270.
Kuida, K., 2000. Caspase-9. The International Journal of Biochemistry & Cell Biology 32, 121–124.
Lin, S.J., Shyue, S.K., Liu, P.L., Chen, Y.H., Ku, H.H., Chen, J.W., Tam, K.B., Chen, Y.L., 2004. Adenovirus-mediated overexpression of catalase attenuates oxLDL-induced apoptosis in human aortic endothelial cells via AP-1 and C-Jun N-terminal kinase/extracellular signal-regulated kinase mitogen-activated protein kinase pathways. Journal of Molecular and Cellular Cardiology 36, 129–139.
Liu, C.L., Xie, L.X., Li, M., Durairajan, S.S., Goto, S., Huang, J.D., 2007. Salvianolic acid B inhibits hydrogen peroxide-induced endothelial cell apoptosis through regulating PI3K/Akt signaling. PLoS One 2, e1321.
Matés, J.M., Sánchez-Jiménez, F., 1999. Antioxidant enzymes and their implications in pathophysiologic processes. Frontiers in Bioscience 4, 339–345.
McNally, J.S., Davis, M.E., Giddens, D.P., Saha, A., Hwang, J., Dikalov, S., Jo, H., Harrison, D.G., 2003. Role of xanthine oxidoreductase and NAD(P)H oxidase in endothelial superoxide production in response to oscillatory shear stress. American Journal of Physiology, Heart and Circulatory Physiology 285, 2290–2297.
Muñoz, C., Castellanos, M.C., Alfranca, A., Vara, A., Esteban, M.A., Redondo, J.M., de Landázuri, M.O., 1996. Transcriptional up-regulation of intracellular adhesion molecule-1 in human endothelial cells by the antioxidant pyrrolidine dithiocarbamate involves the activation of activating protein-1. Journal of Immunology 157, 3587–3597.
Nohl, H., Kozlov, A.V., Gille, L., Staniek, K., 2003. Cell respiration and formation of reactive oxygen species: facts and artefacts. Biochemical Society Transactions 31, 1308–1311.
Ryter, S.W., Alam, J., Choi, A.M., 2006. Heme oxygenase-1/carbon monoxide: from basic science to therapeutic applications. Physiological Reviews 86, 583–650.
St-Pierre, J., Drori, S., Uldry, M., Silvaggi, J.M., Rhee, J., Jäger, S., Handschin, C., Zheng, K., Lin, J., Yang, W., Simon, D.K., Bachoo, R., Spiegelman, B.M., 2006. Suppression of reactive oxygen species and neurodegeneration by the PGC-1 transcriptional coactivators. Cell 127, 397–408.
Takahama, K., Miyata, T., 1995. Cough-diversity and the peripheral mechanisms of production. Folia Pharmacologica Japonica 105, 41–52.
Usatyuk, P.V., Vepa, S., Watkins, T., He, D., Parinandi, N.L., Natarajan, V., 2003. Redox regulation of reactive oxygen species-induced p38 MAP kinase activation and barrier dysfunction in lung microvascular endothelial cells. Antioxidants & Redox Signaling 5, 723–730.
Valen, G., Erl, W., Eriksson, P., Wuttge, D., Paulsson, G., Hansson, G.K., 1999. Hydrogen peroxide induces mRNA for tumour necrosis factor alpha in human endothelial cells. Free Radical Research 31, 503–512.
Varani, J., Dame, M.K., Gibbs, D.F., Taylor, C.G., Weinberg, J.M., Shayevitz, J., Ward, P.A., 1992. Human umbilical vein endothelial cell killing by activated neutrophils. Loss of sensitivity to injury is accompanied by decreased iron content during in

vitro culture and is restored with exogenous iron. Laboratory Investigation 66, 708–714.
Wang, J., Shen, Y.H., Utama, B., Wang, J., LeMaire, S.A., Coselli, J.S., Vercellotti, G.M., Wang, X.L., 2006. HCMV infection attenuates hydrogen peroxide induced endothelial apoptosis—involvement of ERK pathway. FEBS Letters 580, 2779–2787.
Watanabe, N., Zmijewski, J.W., Takabe, W., Umezu-Goto, M., LeGoffe, C., Sekine, A., Landar, A., Watanabe, A., Aoki, J., Arai, H., Kodama, T., Murphy, M.P., Kalyanaraman, R., Darley-Usmar, V.M., Noguchi, N., 2006. Activation of mitogen-activated protein kinases by lysophosphatidylcholine-induced mitochondrial reactive oxygen species generation in endothelial cells. American Journal of Pathology 168, 1737–1748.
Yang, B.H., Oo, T.N., Rizzo, V., 2006. Lipid rafts mediate H_2O_2 prosurvival effects in cultured endothelial cells. FASEB Journal 20, 688–697.
Yang, J.Y., Michod, D., Walicki, J., Widmann, C., 2004. Surviving the kiss of death. Biochemical Pharmacology 68, 1027–1031.
Zafari, A.M., Ushio-Fukai, M., Akers, M., Yin, Q., Shah, A., Harrison, D.G., Taylor, W.R., Griendling, K.K., 1998. Role of NADH/NADPH oxidase-derived H_2O_2 in angiotensin II-induced vascular hypertrophy. Hypertension 32, 488–495.